PPS
Paper
www.rsc.org/pps

A time-resolved study of concentration quenching of disulfonated aluminium phthalocyanine fluorescence †

Zdeněk Petrášek and David Phillips*

Department of Chemistry, Imperial College of Science, Technology and Medicine, London, United Kingdom SW7 2AY

Received 9th October 2002, Accepted 9th November 2002
First published as an Advance Article on the web 27th January 2003

The effects of concentration on the fluorescence decay kinetics of disulfonated aluminium phthalocyanine ($AlPcS_2$) were studied in several solvents. The degree of aggregation, which increased with total dye concentration, was estimated from the absorption spectra. The measured fluorescence decays were shorter and increasingly non-monoexponential with increasing dye concentration. However, stronger quenching was not correlated with higher aggregation. The fluorescence decays were analyzed using a model that assumes excitation energy migration between diffusing monomeric $AlPcS_2$ and quenching by diffusing dimers, both governed by the Förster energy transfer mechanism. The model can explain the observations in three of the four solvents used (phosphate-buffered saline (PBS) pH = 11.5, ethanol, and 67% glycerol–33% water mixture) on the assumption that different dimer configurations are present and not all of them act as quenchers. In PBS at pH = 7.4 the theory predicts much stronger quenching than observed. Excitation energy migration between monomeric species at high dye concentration was confirmed by the observed decrease of the decay time of fluorescence anisotropy in viscous solutions of 67% glycerol, and appears to be a major factor in fluorescence quenching of $AlPcS_2$ at high concentration.

Introduction

Disulfonated aluminium phthalocyanine ($AlPcS_2$, Fig. 1)

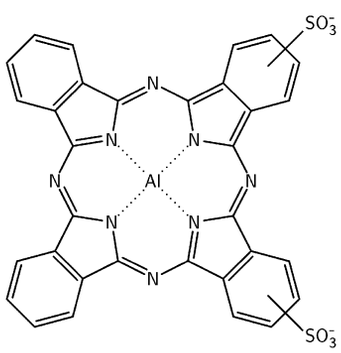

Fig. 1 Structure of disulfonated aluminium phthalocyanine ($AlPcS_2$).

studied in this work is used as a drug in photodynamic therapy (PDT).[1] The applicability and efficacy of a PDT drug can be linked to its photophysical properties, such as quantum yields of fluorescence, triplet state formation and singlet oxygen formation. The photophysics of potential drugs are usually first studied in homogeneous solutions, and on the basis of the established parameters their photosensitizing potential is predicted or explained. However, when located in cells and tissues, the sensitiser is interacting with many types of molecules and cellular components, and its surrounding environment is far from homogeneous. For this reason the photophysics of sensitisers are often studied in various model heterogeneous systems, such as micelles or liposomes.

The photophysical processes of sulfonated aluminium phthalocyanines in homogeneous media have been studied previously.[1–3] $AlPcS_2$ in buffered aqueous solution at pH = 7.4 is characterized by fluorescence quantum yield $\Phi_F = 0.40$, triplet quantum yield $\Phi_T = 0.17$ and singlet oxygen quantum yield $\Phi_\Delta = 0.17$. The fluorescence decay is monoexponential with a lifetime of 5.0 ns. The aggregates of $AlPcS_2$ were found to be non-fluorescent.[4] In more complex systems, such as reversed micelles,[5,6] liposomes,[7,8] and living cells[9] the photophysics of $AlPcS_2$ is more complex and depends on the dye concentration. The local dye concentration in these heterogeneous systems can achieve much higher values than the concentration of a bulk solution. In general, the quantum yields of fluorescence and triplet formation were found to decrease with increasing dye concentration. Fluorescence decays in these systems are often not monoexponential, and their decay rate increases with increasing concentration. It has been suggested that this concentration dependence is a consequence of an interaction of phthalocyanine molecules in close proximity (energy transfer, electron transfer) resulting in self-quenching. Aggregation is expected to play an important role at high dye concentration, and dimers or statistical pairs (two molecules in close proximity) were suggested to act as fluorescence quenchers.[7,9]

Concentration quenching of other dyes, sulforhodamine 101[10] and 5(6)-carboxyfluorescein,[11] was studied previously by incorporating the dye into liposomes. The reason for using liposomes was not to model biological assemblies, but to obtain high local dye concentrations while the absorption of the whole sample remains low, and thus to avoid fluorescence reabsorption. It was found that the fluorescence intensity and fluorescence lifetimes decrease with increasing dye concentration. At higher dye concentrations the decays were not monoexponential and were fitted to 2–3 exponentials. The observations were explained as a consequence of dimerization (static quenching) and excitation energy transfer to dimer (dynamic quenching) facilitated by energy migration between monomers. The observed fluorescence depolarization provided evidence for direct Förster energy transfer between monomers.[11]

Scully *et al.*[12] used time resolved fluorescence spectroscopy to study excitation energy transfer in solutions of high dye concentration. The observed fluorescence decays, which were non-exponential and faster with increasing dye concentration, were

† Dedicated to Professor Jean Kossanyi on the occasion of his 70th birthday.

 DOI: 10.1039/b209906c

described using Förster and LAF (Loring, Anderson, Fayer) models. The quenching of the dye (Rhodamine 6G) by added quencher molecules or by dimers was enhanced by excitation energy migration between monomers. Nakamura *et al.*[13] observed similar enhancement of fluorescence quenching by oxygen at high dye (chlorophyll a) concentration. The diffusion of reacting molecules was not taken into account in either of these two studies.

In this work the effects of high concentration and aggregation on the fluorescence decay kinetics of $AlPcS_2$ in homogeneous solutions were studied. The aim was to find a model describing the observed fluorescence decays, to characterize the interactions between dye molecules in the systems investigated, and to discuss possible implications of the results on the use of $AlPcS_2$ as a photosensitiser of PDT.

Theory of fluorescence quenching

Bimolecular fluorescence quenching can be described as an interaction between a fluorescent molecule in the excited state and a quencher molecule, which results in dissipation of the excitation energy *via* non-radiative pathways, so that no photon is emitted. The rate of quenching, which is generally time-dependent, is determined by two factors: the rate of diffusion bringing the fluorescent molecule and the quencher near each other so that they can react, and the rate of the quenching reaction itself. If the intrinsic reaction rate is infinitely fast compared to the rate of diffusion, the reaction is fully diffusion controlled. The other extreme is the case of a very low intrinsic reaction rate relative to diffusion or a situation where diffusion is suppressed, such as in frozen solutions or in solutions of high viscosity. Then the fluorescence quenching is diffusion-independent.

Smoluchowski solved the diffusion equation and obtained an expression for the fluorescence decay of the quenched molecule (eqn. 1) in the condition that the fluorescent molecule and quencher react with infinite reaction rate when the distance between them reaches the limiting value of R[14].

$$I(t) = I(0)e^{-bt-c\sqrt{t}} \tag{1}$$

$I(0)$ is the fluorescence intensity at time $t = 0$. The parameters b and c depend on the reaction distance R, the sum of diffusion coefficients of the fluorescent molecule and the quencher D, and the quencher concentration [Q] as expressed by eqns. 2 and 3:

$$b = 1/\tau_0 + 4\pi RDN_A[\mathrm{Q}] \tag{2}$$

$$c = 8\sqrt{\pi D}R^2N_A[Q] \tag{3}$$

where τ_0 is the fluorescence lifetime of the fluorescent molecule in the absence of quencher and N_A is the Avogadro number ($N_A = 6.022 \times 10^{23}$). Using these equations, R and D can be calculated from parameters b and c determined from fits to experimental fluorescence decays. The calculated diffusion coefficient D can be compared with the theoretical value for a spherical particle of diameter a in solution of viscosity η:

$$D = \frac{kT}{6\pi\eta a} \tag{4}$$

In some cases the term $-c\sqrt{t}$ in the exponent of eqn. 1 can be neglected, the reaction rate $k = 1/\tau_0 + 4\pi RDN_A[\mathrm{Q}]$ becomes time-independent, and the fluorescence decay monoexponential. This is the most commonly used classical kinetics approximation.[14]

The Smoluchowski theory was modified by Collins and Kimball (SCK theory) to take into account the finite rate k_r of the quenching reaction.[14] In the long-time approximation the fluorescence decay is again described by eqn. 1, however with modified parameters b and c. Similarly, when interaction between ionic reactants are taken into account (Debye–SCK theory[14]) or when diffusion dependent quenching in two-dimensional systems is studied[15] the fluorescence decay can be approximated by eqn. 1 with modified parameters b and c.

All the so far mentioned models assume that the quenching reaction occurs at a single boundary (when the distance between reactants is R) with a constant reaction rate. A more realistic assumption is a position dependent reaction rate $k(R)$, since, for example, energy transfer in a dipole–dipole approximation displays a $1/R^6$ dependence and electron transfer decreases exponentially with increasing reaction distance R[16].

A model assuming quenching by direct Förster energy transfer and fixed positions of donors and acceptors (no diffusion) predicts fluorescence decay in the form of eqn. 1. The parameters b and c depend on fluorescence lifetime in the absence of acceptors τ_0 and acceptor concentration c_A in the following way:

$$b = \frac{1}{\tau_0},\ c = \frac{4}{3}\gamma\pi^{3/2}N_Ac_AR_{DA}^3\tau_0^{-1/2} \tag{5}$$

where γ is related to the orientation factor κ and has a value of 1 for infinitely rapid molecular reorientation and a value of 0.845 for fixed molecular orientation. Note that in this case the parameter b does not depend on the acceptor (quencher) concentration. The rate of energy transfer $k_{D \longrightarrow A}$ between donor and acceptor molecules separated by distance R is described by eqn. 6:

$$k_{D\to A}(R) = \frac{1}{\tau_r}\left(\frac{R_{DA}}{R}\right)^6 \tag{6}$$

where τ_r is radiative fluorescence lifetime of the donor and R_{DA} is the critical transfer distance:

$$R_{DA}^6 = \frac{9\ln 10\kappa^2\Phi_D^0}{128\pi^5n^4N_A}\int_0^\infty \frac{J_{fD}(\tilde{\nu})\varepsilon_A(\tilde{\nu})}{\tilde{\nu}^4}d\tilde{\nu} \tag{7}$$

$J_{fD}(\tilde{\nu})$ is the normalized fluorescence spectrum of the donor, $\varepsilon_A(\tilde{\nu})$ is the decadic molar absorption coefficient of the acceptor, $\tilde{\nu}$ is the wavenumber, n is the refractive index of the solvent, and Φ_D^0 is the fluorescence quantum yield of the donor. This model assumes immobile donors and acceptors and is therefore applicable to rigid media or low viscosity solutions. Another assumption is a low concentration of donors, so that no energy migration between donors is possible.

Jang *et al.*[17] developed a theory of fluorescence quenching that takes into account diffusion of both donors and acceptors, migration of excitation energy between donors, and assumes a Förster energy transfer mechanism. The approximate expression for a fluorescence decay has a form of eqn. 1 where:

$$b = 1/\tau_0 + 4\pi\sigma_F D_{eff}N_Ac_A = A + B \times c_A \tag{8}$$

$$c = \frac{4}{3}\pi^{3/2}R_{DA}^3\tau_0^{-1/2}N_Ac_A = C \times c_A \tag{9}$$

D_{eff} is an effective diffusion coefficient:

$$D_{eff} = D_T + \frac{2\pi R_{DD}^6c_D}{3r_c\tau_0} \tag{10}$$

where D_T is the relative translational diffusion coefficient between donors and acceptors, and R_{DD} is the critical transfer

distance between donors. Distances r_c (cutoff distance introduced in order to exclude nonphysical self-transfer in the mathematical description of donor-to-donor excitation migration) and σ_F (related to R_{DA}) are defined in ref. 17. D_{eff} is higher than sum of D_T and D_E, the excitation-migration diffusion coefficient calculated for a system with immobile donors and acceptors, as supported by earlier experiments.[18] The coefficient D_E is defined as $D_E = \alpha(4\pi c_D R^3_{DD}/3)^{4/3} (R^2_{DD}/\tau_0)$, where α is a constant which depends on the theory applied.[17] The increase in quenching due to excitation energy transfer is therefore higher than that predicted by theories where D_{eff} is taken as a simple sum of D_T and D_E.

Fluorescence anisotropy

A useful method for studying radiationless energy transfer is the measurement of fluorescence depolarization. Energy transfer preceding the emission results in lower fluorescence anisotropy. For example, in a hypothetical case where emission of every photon is preceded by exactly one act of energy transfer from the originally excited molecule the fluorescence anisotropy is reduced to 1/25 of its initial value[19] when the average over all possible donor and acceptor orientations is considered. The rate of decay of fluorescence anisotropy in the presence of radiationless energy transfer then depends not only on the rotation of the molecules during their existence in the exited state but also on the rate of excitation energy transfer. If the contribution of rotational depolarization mechanisms can be neglected (for example in the case of viscous solutions) the fluorescence anisotropy decay provides a direct measure of excitation energy transfer.

The fluorescence intensity components polarized parallel ($I_{||}(t)$) and perpendicular ($I_{\perp}(t)$) to the polarization of the excitation light are related to the total fluorescence intensity $I(t) = I_{||}(t)+2I_{\perp}(t)$ and the decay of fluorescence anisotropy a(t) in the following way:

$$I_{||}(t) = \frac{1}{3} I(t)(1 + 2a(t)) \quad (11)$$

$$I_{\perp}(t) = \frac{1}{3} I(t)(1 - a(t)) \quad (12)$$

The decay of fluorescence anisotropy due to rotational diffusion of a spherical particle is expressed by eqn. 13:

$$a(t) = a_0 e^{-t/\tau_R} \quad (13)$$

where τ_R is the rotational correlation time and a_0 the initial anisotropy. Then, the time dependence of fluorescence intensity components $I_{||}(t)$ and $I_{\perp}(t)$ can be expressed as:

$$I_{||,\perp}(t) = \frac{1}{3} I(t)(1 + g_{||,\perp} e^{-t/\tau_R}) \quad (14)$$

where $g_{||} = 2a_0$ and $g_{\perp} = -a_0$. The presence of energy transfer manifests itself by a change in the parameter τ_R in eqns. 13 and 14 or by change in the decay law of fluorescence anisotropy (eqn. 13).

Experimental

$AlPcS_n$ were prepared according to the method of Ambroz *et al.*[20] and separated into mono-, di-, tri- and tetrasulfonated species by medium-pressure chromatography. The $AlPcS_2$ synthesised by this procedure consists predominantly of the α,α-*cis*-isomer. The photophysics of the various structural isomers of $AlPcS_2$ have been separately investigated, and found to be essentially identical.

Absorption spectra were measured using a Lambda 2 Perkin-Elmer spectrometer. The spectra of the concentrated phthalocyanine solutions were measured in a 0.01 mm pathlength cuvette because of high absorbance values.

Fluorescence decays were recorded using the time-correlated single photon counting (TCSPC) technique.[21] A Coherent 590–03/7220 dye laser pumped by the green line (532 nm) of a frequency-doubled mode-locked Coherent Antares 76-s laser provided the excitation pulses. The excitation wavelength was 640 nm and the fluorescence was detected at 680 nm, which is the position of the fluorescence maximum of the emitting species, the $AlPcS_2$ monomer. The dye laser was pumped at a frequency of 76 MHz, and this was reduced to 3.8 MHz by a cavity dumper. Fluorescence from the sample was detected by a microchannel plate photomultiplier tube Photek PMT 413LJ. The samples were measured in a 0.1 mm pathlength cuvette and front face (0°) excitation/detection configuration was used. This was accomplished by placing a beamsplitter in front of the cuvette between the cuvette and the monochromator. Before detection fluorescence was passed through a polarizer oriented at the magic angle of 54.7°. Fluorescence decays were recorded so that the number of counts in the peak channel was 5000–20000 depending on the fluorescence intensity. The instrument response function (IRF) was recorded using a Ludox scattering solution. A typical width of IRF was less than 100 ps at FWHM. Fluorescence decays were analyzed by iterative reconvolution method. The goodness of the fit was judged by the value of χ_r^2 (the least-squares method). For the minimization of χ_r^2 the Levenberg–Marquardt algorithm was used.[21] When the decay of fluorescence anisotropy was investigated two decays for every sample were recorded, with the polarizer oriented at 0° and 90° respectively. The two decays were then analyzed globally employing eqn. 14.

Results

In order to study the fluorescence decay kinetics at high concentration, solutions of $AlPcS_2$ in the concentration range 0.5–20 mM in PBS (pH = 7.4 and 11.5), ethanol and 67% glycerol–33% water were used. The measured absorption spectra are shown in Fig. 2. All solutions showed a high degree of aggregation and variations in the absorption profile with solvent and concentration.

If it is assumed that the samples contain only monomers and dimers and that the concentrations of these species are determined by equilibrium characterized by dimerization constant K (see eqn. 16 in the Appendix), it is possible to calculate monomer and dimer concentrations and absorption spectra from the experimental spectra. This method is described in the Appendix.

The monomer and dimer spectra of $AlPcS_2$ in PBS at pH = 7.4 were calculated in this way (Fig. 3). The recovered value of K was $1.4 \pm 0.2 \times 10^5$ M^{-1}. This method failed when applied to the absorption spectra of $AlPcS_2$ in the other three solvents; the calculated spectra contained either negative values or sharp peaks which are unlikely to exist in real spectra. This is most likely due to the presence of higher order aggregates and therefore invalidates eqns. 15–17 (see Appendix). The concentrations of monomer and dimer in these samples were estimated from the absorption spectra assuming that the absorbance at 720 nm originates only from the dimer, and that the dimer absorbance at 720 nm is approximately equal to the dimer absorbance at 670 nm. These additional assumptions are based on the calculated spectral shapes of monomer and dimer in PBS at pH = 7.4 (Fig. 3). Solving eqns. 15 and 17 for these two wavelength values (670 and 720 nm) provided the estimates of the sought concentrations. The calculated monomer and dimer concentrations of $AlPcS_2$ in the four solvents used are shown in Fig. 4. The monomer and dimer concentrations indicate that the tendency of $AlPcS_2$ to aggregate depending on the solvent increases in

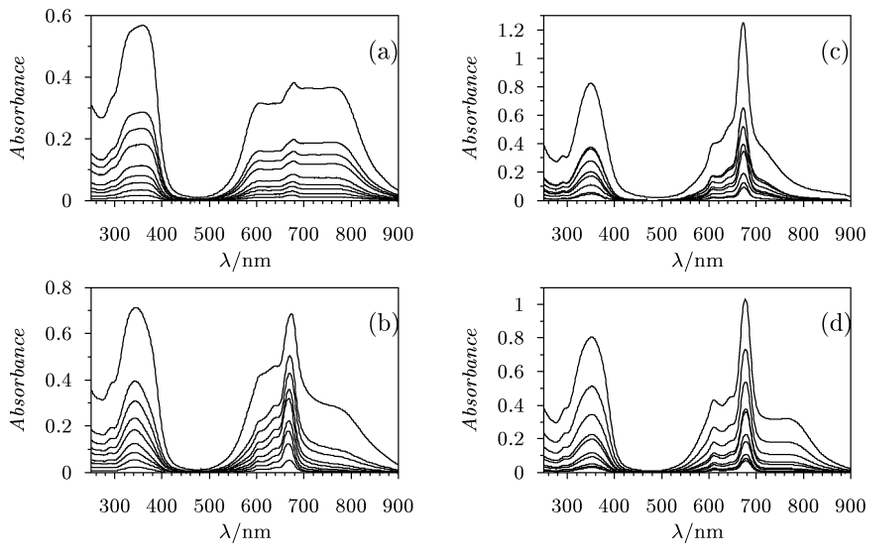

Fig. 2 Absorption spectra of $AlPcS_2$ in concentration range 0.5–20 mM in four different solvents: (a) PBS pH = 7.4, (b) PBS pH = 11.5, (c) ethanol, (d) 67% glycerol–33% water. The concentrations of PBS and ethanol solutions (a–c) are 0.5, 1, 2, 3, 4, 6, 8, 10, and 20 mM. The concentrations of glycerol solutions (d) are the same as those in Table 2. The absorption values increase with increasing concentration in all cases. The monomer band at ~670 nm is overlapped by a broad dimer band in the 560–840 nm region (see also Fig. 3).

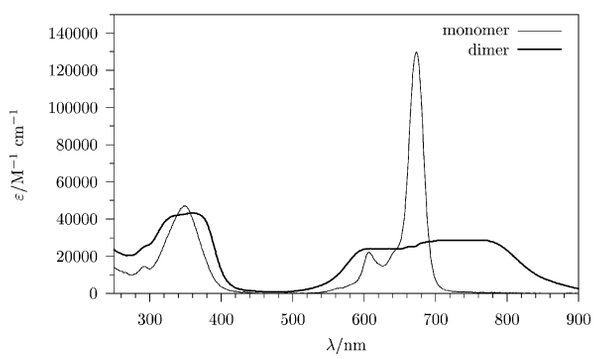

Fig. 3 Calculated absorption spectra of $AlPcS_2$ monomer and dimer in PBS at pH = 7.4. The spectra were calculated from the experimental absorption spectra of $AlPcS_2$ in PBS at pH = 7.4 (Fig. 2a) assuming equilibrium between monomer and dimer species (eqns. 15–17) using the method described in the Appendix.

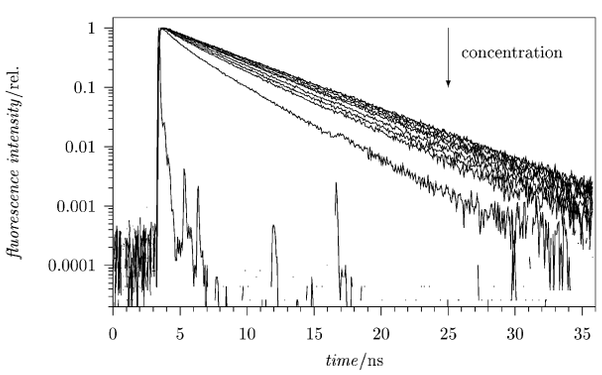

Fig. 5 Fluorescence decays of $AlPcS_2$ in PBS pH = 7.4. The concentrations are: 0.5, 1, 2, 3, 4, 6, 8, 10, and 20 mM. The excitation wavelength was 640 nm and the fluorescence was detected at 680 nm.

the following order: 67% glycerol–33% water < ethanol < PBS pH = 11.5 < PBS pH = 7.4.

The fluorescence decays of $AlPcS_2$ in all used solvents are shown in Figs. 5–8. The decays, which are apparently not monoexponential, were fitted to a two-exponential function and to eqn. 1. The analysis using both functions resulted in fits of similar quality (χ_r^2 < 1.5, with the exception of the highest

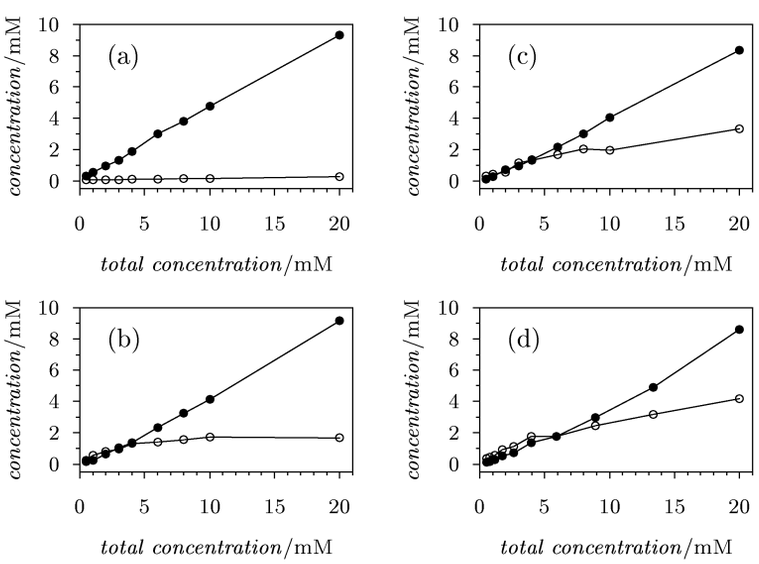

Fig. 4 Concentrations of $AlPcS_2$ monomer (○) and dimer (●) as determined from the absorption spectra. Solvents: (a) PBS pH = 7.4, (b) PBS pH = 11.5, (c) ethanol, (d) 67% glycerol–33% water. The concentrations in case (a) were calculated as described in the Appendix. The concentrations in the other cases were estimated from the absorption spectra (Fig. 2b–d) as described in the text.

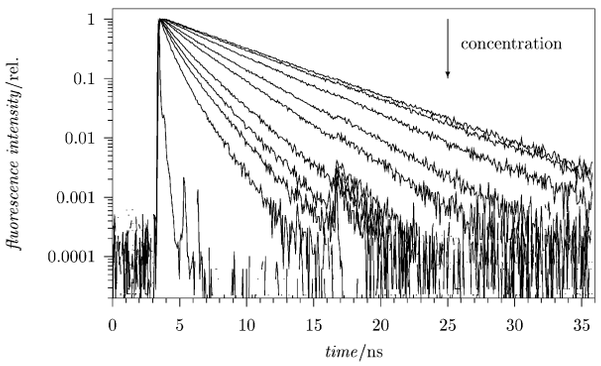

Fig. 6 Fluorescence decays of $AlPcS_2$ in PBS pH = 11.5. The concentrations are: 0.5, 1, 2, 3, 4, 6, 8, 10, and 20 mM. The excitation wavelength was 640 nm and the fluorescence was detected at 680 nm.

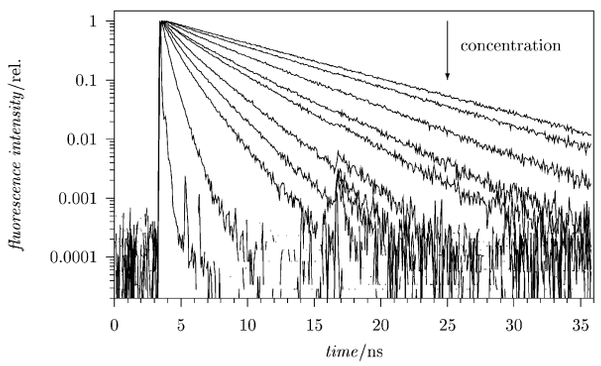

Fig. 7 Fluorescence decays of $AlPcS_2$ in ethanol. The concentrations are: 0.5, 1, 2, 3, 4, 6, 8, 10, and 20 mM. The excitation wavelength was 640 nm and the fluorescence was detected at 680 nm.

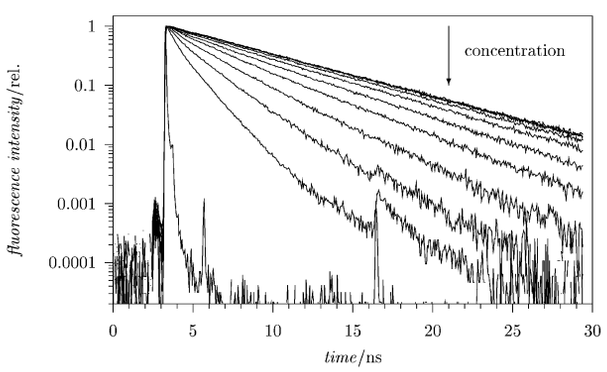

Fig. 8 Fluorescence decays of $AlPcS_2$ in 67% glycerol–33% water. The concentrations are: 0.52, 0.78, 1.2, 1.8, 2.6, 4, 5.9, 8.9, 13, and 20 mM. The excitation wavelength was 640 nm and the fluorescence was detected at 680 nm.

concentration). The two-exponential fits yielded lifetimes varying with the total dye concentration in the range τ_1 = 0.2–3.2 ns and τ_2 = 0.6–7.3 ns with the pre-exponential factors also depending on the total concentration.

The parameters b and c from fits to eqn. 1 exhibit linear dependence on dimer concentration c_d and also on the total concentration c_{tot} suggesting that dimer acts as a quencher. The dependence of b and c on the monomer concentration c_m deviates from linearity. Therefore, the parameters b and c were fitted to eqns. 8 and 9 with dimer as a quencher. The calculated values of A, B and C are shown in Table 1.

The fluorescence decays of $AlPcS_2$ in 67% glycerol–33% water were also measured with the emission polarizer oriented parallel and perpendicular to the polarization of the excitation light, in order to investigate the decay of fluorescence anisotropy. The decays were analyzed globally ($I_{||}$ and $I_{\perp}$ of one concentration together) using eqn. 14 where the fluorescence

Table 1 Parameters A, B and C recovered from analysis of fluorescence decays of $AlPcS_2$ and defined by eqns. 8 and 9, and parameter f defined in the text

Solvent	$A/10^8$ s^{-1}	$B/10^{10}$ M^{-1} s^{-1}	$C/10^6$ M^{-1} s$^{-1/2}$	f
PBS pH = 7.4	1.90	0.274	1.65	60
PBS pH = 11.5	1.80	7.20	7.05	3.5
Ethanol	1.20	8.72	7.91	2
67% Glycerol	1.51	3.56	3.43	9

Table 2 The decay time of fluorescence anisotropy τ_R and parameters $g_{||}$ and $g_{\perp}$ from eqn. 14 recovered from analysis of fluorescence decays of $AlPcS_2$ in 67% glycerol–33% water

	Eqn. 14		
$AlPcS_2$ conc./mM	τ_R/ns	$g_{||}$	$g_{\perp}$
0.52	3.7	0.196	−0.052
0.78	3.6	0.186	−0.050
1.2	3.1	0.176	−0.049
1.8	2.6	0.176	−0.048
2.6	2.4	0.160	−0.049
4.0	1.9	0.155	−0.040
5.9	1.4	0.155	−0.041
8.9	0.86	0.156	−0.033
13	0.87	0.148	−0.027
20	0.65	0.118	−0.024

anisotropy decay is approximated by a monoexponential function. The value of the time constant τ_R decreased with increasing $AlPcS_2$ concentration (Table 2). The value of τ_R for dilute solution, where no interaction between solute molecules is expected, was measured to be τ_R = 5.0 ns and the value of initial anisotropy a_0 was found to be 0.1.

The experimentally obtained parameters b and c were compared with the predictions based on the theory by Jang *et al.*.[17] For this purpose the Förster critical transfer distances R_{DD} and R_{DA} for energy transfer between monomers and monomer and dimer, respectively, were calculated from eqn. 7 using the absorption spectrum of the monomer in Fig. 3. The values obtained are: R_{DD} = 6.88 nm and R_{DA} = 5.98 nm. The fluorescence quantum yield of $AlPcS_2$ is 0.4[6]. As τ_0 the experimental value $1/A$ (Table 1) was used. The contact distances σ and σ_d were estimated as 2 nm. The diffusion coefficient of monomer D_T was calculated as $D_T = 1.42D$, where D was calculated from eqn. 4 where a was set to 1 nm, and 1.42 is a correction for the fact that the phthalocyanine molecule is not a sphere. The value of 1.42 was obtained assuming the shape of an oblate ellipsoid with the main axis 5 times shorter than the other axis.[22] The diffusion coefficient of dimer was set to be the same as that of monomer. It was found that the value of dimer diffusion coefficient has a negligible effect on the calculated values of parameters b and c.

The parameters b and c obtained in this way were always greater than the experimental values and therefore predicted a faster decay. The difference between experimental and calculated values increased with dye concentration and at the highest concentration the predicted values were 2–8 times higher than the experimental, depending on the solvent.

This discrepancy can be resolved by assuming that the samples contain dimers of different configurations (as shown by Ostler and co-workers[23,24]) and by realizing that only dimers of certain configuration (those having a significant overlap between the absorption spectrum and the emission spectrum of the monomer) can act as energy acceptors (quenchers). Let us assume, for example, that the sample contains two types of dimer, both at the same concentration with different absorption spectra, and that only absorption spectrum of one dimer has a non-zero overlap with the monomer emission spectrum. Then, the acceptor concentration used in the calculation of b and c

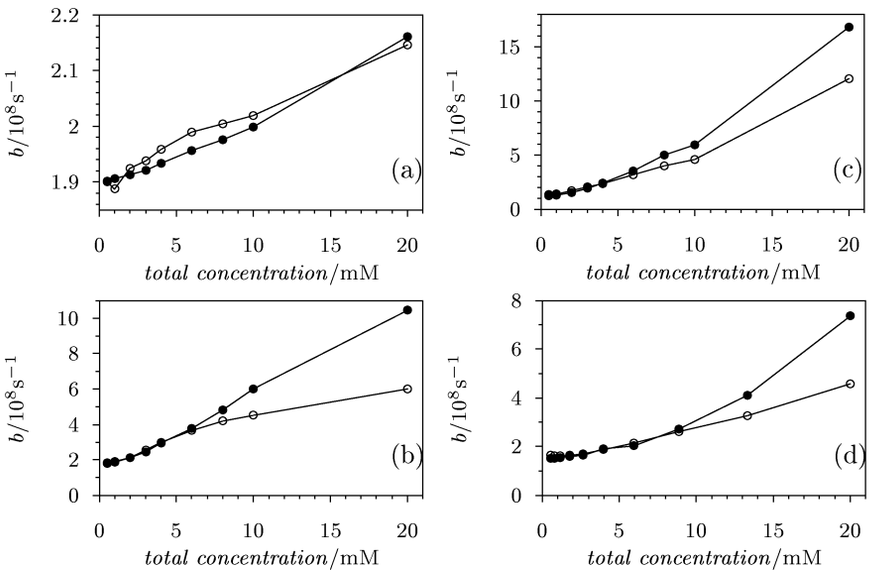

Fig. 9 Experimental (○) and calculated (●)(eqn. 8) values of parameter b (eqn. 1). The experimental values were obtained from the fits of the fluorescence decays (Figs. 5–8) to eqn. 1. Solvents: (a) PBS pH = 7.4, (b) PBS pH = 11.5, (c) ethanol, (d) 67% glycerol–33% water.

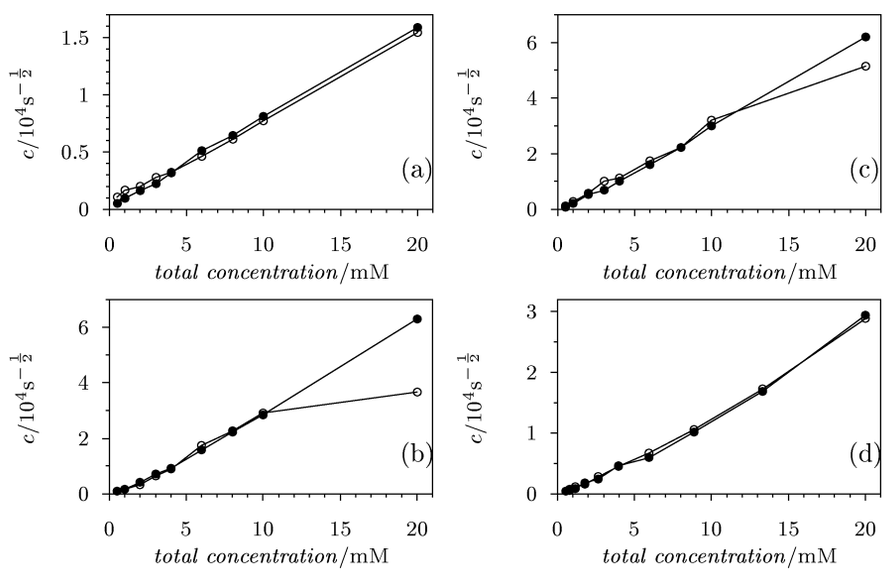

Fig. 10 Experimental (○) and calculated (●)(eqn. 9) values of parameter c (eqn. 1). The experimental values were obtained from the fits of the fluorescence decays (Figs. 5–8) to eqn. 1. Solvents: (a) PBS pH = 7.4, (b) PBS pH = 11.5, (c) ethanol, (d) 67% glycerol–33% water.

will be half of the total dimer concentration. Furthermore, the molar absorption coefficient of the quenching dimer used to calculate R_{DA} will be twice the previously considered value because the same absorbance value must be obtained in order to agree with the experimental absorption spectra. The change of the molar absorption coefficient will lead toan increase in R_{DA} by a factor of $2^{1/6}$ according to eqn. 7. If the sample contains f different types of dimer with only one of them acting as a quencher of monomer fluorescence then the quencher concentration used to calculate b and c will change to c_a/f and the critical transfer distance will change to $R_{DA} \cdot f^{1/6}$.

It was possible to find an effective value of f for every solvent used to match reasonably well the values of b and c calculated according to Jang *et al.* with the experimental values. The values of f are shown in Table 1 and b and c in Figs. 9 and 10, together with the experimental values.

Discussion

The variation in the spectral shapes of $AlPcS_2$ dimer between PBS solvents of different pH is in agreement with the findings of Ostler *et al.*[23,24] who suggested the existence of two or more types of $AlPcS_2$ dimer. The two co-facial dimer structures proposed by Ostler contain Cl^- or OH^- as a bridging ligand between participating monomers, and each monomer has one axial ligand: H_3O^+ or H_2O, respectively. The observed different positions and shapes of absorption bands of dimers are thought to be a consequence of the varying dimer configuration and composition with solvent. Moreover, the broad shape of the recovered dimer spectrum of the solution in PBS pH = 7.4 suggests that more dimer configurations with shifted absorption bands are present at the same time. The calculated dimer spectrum then does not represent an absorption spectrum of one dimer species, but is rather an effective dimer spectrum composed of the spectra of dimers with statistically distributed configurations,[25] as exemplified by eqn. 26.

An important observation can be made by comparing the time-resolved fluorescence data in different solvents (Figs. 2, 5–8): although the concentration of dimer, the supposed quencher, varies only a little for a given total $AlPcS_2$ concentration, the variation in the quenching efficiency is much greater. In fact, the quenching efficiency increases while the dimer concentration is slightly decreasing. The increase in quenching is correlated with the increase in monomer concen-

tration (for a given total concentration), which means that some kind of monomer–monomer interaction is involved in fluorescence quenching. The only exception is the solution of $AlPcS_2$ in glycerol, where less quenching is observed than in ethanol and PBS at pH = 11.5, and which aggregates least. An obvious explanation is the involvement of molecular diffusion in fluorescence quenching. The viscosity η of 67% glycerol–33% water is higher (η = 16 cP [26]) than that of the other solvents, therefore the rate of quenching due to molecular diffusion in glycerol is expected to be lower.

A higher concentration of monomers means a lower mean distance between the molecules and therefore more efficient energy migration, as follows from eqn. 6. A single energy transfer act produces on average a 25-fold decrease in anisotropy, that is a decrease to $a = 0.004$ in the case of $AlPcS_2$.[19] Multiple energy transfers occurring before the photon emission cause further lowering of the fluorescence anisotropy. The observed decrease in the fluorescence anisotropy decay time with increasing dye concentration (Table 2) can then be interpreted as an increase in the efficiency of excitation energy transfer between monomers. The fluorescence anisotropy decay time of dilute $AlPcS_2$ solution (τ_R = 5.0 ns) originates fully from rotational depolarization.

According to the theory of fluorescence depolarization, the value of the initial fluorescence anisotropy of a solution excited with linearly polarized light is in the simplest case 0.4. However, this is not the case for $AlPcS_2$ where the first excited state, from which the emission occurs, is degenerate. The first excited state consists of two states with transition dipole moments of the same size oriented perpendicularly to each other, and lying in the plane of the ring. Because of the degeneracy of the state the dipole moment of the emission can be any vector lying in the plane of the molecule, not only the transition dipole moment of absorption. Therefore, from the point of view of molecular rotation, the molecule can be regarded as a prolate ellipsoid oriented perpendicularly to the plane of the molecule with rotational relaxation time along the main axis equal to zero. It follows from the theory of fluorescence depolarization by rotational diffusion that the decay of fluorescence anisotropy of such a system is described by a monoexponential function with initial anisotropy $a_0 = 0.1$.[27]

An unexpected result is the decrease of initial anisotropy a_0 ($=g_{||}/2$) with increasing dye concentration, and the fact that experimentally determined $g_{||}$ is not equal to $-2g_{\perp}$. The most probable reason is the approximation of the decay of fluorescence anisotropy by a monoexponential function (eqns. 13 and 14). The anisotropy decay is likely to be non-exponential as the fluorescence decay is, since it is, like fluorescence quenching, determined to a great extent by energy transfer between monomers, and not only by rotational diffusion. The non-spherical shape of the molecule in general also leads to a non-exponential decay of fluorescence anisotropy.

The estimated values of parameter f for $AlPcS_2$ solutions in PBS (pH = 11.5), ethanol and 67% glycerol–33% water are reasonably low and can be interpreted as an effective compensation for various dimer configurations. However, the value of f in PBS (pH = 7.4) solution is too high to explain the differences between predicted and experimental values. It is possible that another mechanism of quenching was present. Beddard *et al.*[28] studied concentration quenching of chlorophyll *a* and suggested quenching by 'statistical pairs', which is two monomer molecules closer than critical distance not interacting in the ground state but forming a non-fluorescent excimer upon excitation of one of the two molecules. Since there is negligible interaction between the molecules in the ground state their existence can not be elucidated from the absorption spectra and their effect on fluorescence quenching is therefore difficult to quantify. Nakamura *et al.*[13] have shown that quenching of chlorophyll *a* by molecular oxygen is enhanced by excitation migration between monomers at high concentration. It is possible that oxygen could account for some of the observed quenching.

In PBS (pH = 7.4) solution the enhancement of quenching by monomer–monomer migration is likely to be low because of low monomer concentration and therefore long intermolecular distances. The fact that the calculated parameters b and c do not agree with experiments could mean that quenching by dimer has been overestimated, possibly because it can not be described by Förster mechanism characterized by R_{DA}. Then the stronger quenching in the other solvents could be explained as energy-migration enhanced quenching by not only dimers but also by 'statistical pairs', molecular oxygen or other molecules which do not quench the $AlPcS_2$ fluorescence appreciably at low concentration.

The fact that the observed degree of quenching was lower than that predicted by Jang's theory [17] could be partially caused by re-emission of reabsorbed fluorescence. Although a very short pathlength cuvette and front configuration was used, the absorption of the samples was high to exclude the possibility of re-emission effects. The re-emission is assumed to be low since the fluorescence absorbed by the dimer, which is in most samples present at higher concentration than the monomer, cannot be re-emitted and therefore cannot contribute to the lengthening of decay. The experimental values of A (Table 1) are lower than those in dilute solutions and could be caused by reemission effects.

Conclusion

The concentration quenching of $AlPcS_2$ has been studied in several solvents. The analysis of absorption spectra showed a variable degree of aggregation in different solvents and provided estimates of monomer and dimer concentrations.

The fluorescence decays of $AlPcS_2$ in all solvents indicate concentration quenching and cannot be described by a monoexponential function. The decays were fitted to eqn. 1 which applies to several models of fluorescence quenching. Since the parameter b is concentration dependent the quenching process cannot be described as pure Förster energy transfer between donors and acceptors. The decrease of fluorescence anisotropy decay time with concentration and the correlation between monomer concentration and degree of quenching at a given total concentration in different solvents both indicate involvement of excitation energy migration between monomers in the fluorescence quenching. The lower quenching in a high viscosity solvent is evidence of the influence of the molecular diffusion.

The parameters obtained from fluorescence decay analysis were compared with Jang's theory [17] assuming that dimer is the quencher. While reasonable agreement was obtained for PBS (pH = 11.5), ethanol and 67% glycerol solvents assuming varying dimer configurations, the prediction for PBS (pH = 7.4) solution suggested much stronger quenching than was observed.

The interpretation of parameters obtained from fits to fluorescence decays is particularly difficult because the concentration of the quencher and, in fact, even the quencher itself are not known with certainty. Previous works on similar molecules suggested quenching by dimers,[13] 'statistical pairs'[28] and oxygen.[13] It seems evident that whatever the quencher, the enhancement of quenching by energy migration between monomers is the crucial factor responsible for the strong quenching at high concentration.

The enhancement of fluorescence quenching means lower quantum yields of fluorescence and triplet state formation. Since the activity of a dye as a photosensitiser depends on the efficiency of formation of the triplet state, the observed enhancement of fluorescence quenching *via* energy migration will lead to lowering of its photosensitizing potential. Furthermore, quenching of the triplet state T_1 by ground state

molecules has been observed previously.[29] At high dye concentrations quenching by ground state molecules will compete with quenching by oxygen, and the result will be a lower singlet oxygen quantum yield, further reducing the photosensitizing efficiency. High local dimer and monomer concentrations combined with high efficiency of direct energy transfer are therefore not desirable for an efficient PDT drug. Unfortunately, the dye concentrations *in vivo* and also the aggregation state are difficult to control since they are influenced by the interaction with the highly heterogeneous intracellular environment and depend on many different parameters.

Appendix

Here, a method of extracting monomer and dimer absorption spectra from a set of experimental absorption spectra of solutions of different concentrations is described.

Assuming equilibrium between monomer and dimer species with dimerization constant K, the following relations describe the system:

$$A(\lambda) = (\varepsilon_{\mathbf{m}}(\lambda)c_{\mathbf{m}} + \varepsilon_{\mathbf{d}}(\lambda)c_{\mathbf{d}})l \tag{15}$$

$$K = \frac{c_{\mathrm{d}}}{c_{\mathrm{m}}^2} \tag{16}$$

$$c_{\mathbf{tot}} = c_{\mathbf{m}} + 2c_{\mathbf{d}} \tag{17}$$

where $A(\lambda)$ is the absorption spectrum, $c_{\mathbf{tot}}$ is the known total $AlPcS_2$ concentration, $c_{\mathbf{m}}$ and $c_{\mathbf{d}}$ monomer and dimer concentrations, $\varepsilon_{\mathbf{m}}(\lambda)$ and $\varepsilon_{\mathbf{d}}(\lambda)$ monomer and dimer extinction coefficients, and l the cuvette pathlength. By applying eqns. 15–17 to the measured absorption spectra, it is possible to calculate the absorption spectra of monomer and dimer $\varepsilon_{\mathbf{m}}(\lambda)$ and $\varepsilon_{\mathbf{d}}(\lambda)$, the concentrations $c_{\mathbf{m}}$ and $c_{\mathbf{d}}$, and the dimerization constant K.

Let us initially assume that the value of K is known. By using eqns. 16 and 17 it is possible to express $c_{\mathbf{m}}$ and $c_{\mathbf{d}}$ as functions of K and $c_{\mathbf{tot}}$, which is also known:

$$c_{\mathrm{m}} = \sqrt{\frac{c_{\mathbf{tot}}}{2K} + \frac{1}{16K^2}} - \frac{1}{4K} \tag{18}$$

$$c_{\mathrm{d}} = \frac{1}{2}\left(c_{\mathbf{tot}} + \frac{1}{4K} - \sqrt{\frac{c_{\mathbf{tot}}}{2K} + \frac{1}{16K^2}} \right). \tag{19}$$

By setting l = 1 and using eqns. 15 and 17 parameters x_λ and y_λ can be defined:

$$A(\lambda) = \frac{\varepsilon_{\mathrm{d}}(\lambda)}{2}c_{\mathbf{tot}} + \left(\varepsilon_{\mathrm{m}}(\lambda) - \frac{\varepsilon_{\mathrm{d}}(\lambda)}{2} \right)c_{\mathrm{m}} \equiv x_\lambda c_{\mathbf{tot}} + y_\lambda c_{\mathrm{m}} \tag{20}$$

Taking individual spectra as multidimensional vectors, the eqn. 20 can be written in a vector form:

$$\mathbf{A} = \mathbf{x}c_{tot} + \mathbf{y}c_{m} \tag{21}$$

and the task of finding $\varepsilon_{\mathbf{m}}(\lambda)$ and $\varepsilon_{\mathbf{d}}(\lambda)$ can be formulated as finding vectors **x** and **y**, and the set of values ${}^{\mathrm{i}}c_{\mathbf{m}}$ that minimize σ_K defined in the following way:

$$\sigma_K = \sum_i \; | \, {}^{\mathrm{i}}\mathrm{A} - \mathrm{x}\, {}^{i}c_{\mathbf{tot}} - \mathrm{y}\, {}^{i}c_{\mathrm{m}} \, |^2 \tag{22}$$

where the sum is taken over all experimentally determined absorption spectra. In order to minimize σ_K we require:

$$\frac{\partial\sigma_K}{\partial x_\lambda} = 0, \; \frac{\partial\sigma_K}{\partial y_\lambda} = 0 \tag{23}$$

Solving eqn. 23 for every λ gives:

$$x_\lambda = \frac{\sum {}^{i}c_{\mathrm{m}}^2 \sum {}^{i}A(\lambda)\,{}^{i}c_{\mathbf{tot}} - \sum {}^{i}c_{\mathbf{tot}}\,{}^{i}c_{\mathrm{m}} \sum {}^{i}A(\lambda)\,{}^{i}c_{\mathrm{m}}}{\sum {}^{i}c_{\mathbf{tot}}^2 \sum {}^{i}c_{\mathrm{m}}^2 - \left(\sum {}^{i}c_{\mathbf{tot}}\,{}^{i}c_{\mathrm{m}} \right)^2} \tag{24}$$

$$y_\lambda = \frac{\sum {}^{i}c_{\mathbf{tot}}^2 \sum {}^{i}A(\lambda)\,{}^{i}c_{\mathrm{m}} - \sum {}^{i}c_{\mathbf{tot}}\,{}^{i}c_{\mathrm{m}} \sum {}^{i}A(\lambda)\,{}^{i}c_{\mathbf{tot}}}{\sum {}^{i}c_{\mathbf{tot}}^2 \sum {}^{i}c_{\mathrm{m}}^2 - \left(\sum {}^{i}c_{\mathbf{tot}}\,{}^{i}c_{\mathrm{m}} \right)^2} \tag{25}$$

where the sums are taken over all measured absorption spectra. The values of ${}^{\mathrm{i}}c_{\mathbf{m}}$ in eqns. 24 and 25 still depend on K, the value of which is unknown. By varying K so that minimum of σ_K is reached one obtains final values for x_λ and y_λ, and therefore $\varepsilon_{\mathbf{m}}(\lambda)$ and $\varepsilon_{\mathbf{d}}(\lambda)$ (*via* eqn. 20), and also sets of $c_{\mathbf{m}}$ and $c_{\mathbf{d}}$ values (*via* eqns. 18 and 19).

If the solutions contain more types of dimers whose equilibria with monomeric species are characterised by dimerisation constants K_a, this method returns an effective dimer spectrum $\varepsilon_{\mathbf{d}}'(\lambda)$ and an effective dimerization constant K'. Using eqns. 15–17 it can be easily shown that the recovered dimer concentration is equal to the sum of the concentrations of all types of dimers, the recovered dimerization constant K' is equal to the sum of the dimerization constants of the individual dimer types, and the obtained effective dimer spectrum $\varepsilon_{\mathbf{d}}'(\lambda)$ is an average of the individual dimer spectra weighed by the dimerization constants K_a. For example, in case of two dimer types with dimerization constants K_1 and K_2 the obtained effective dimer spectrum $\varepsilon_{\mathbf{d}}'(\lambda)$ is related to the individual spectra of the dimers $\varepsilon_{\mathbf{d1}}(\lambda)$ and $\varepsilon_{\mathbf{d2}}(\lambda)$ in the following way:

$$\varepsilon_{\mathrm{d}}'(\lambda) = \frac{K_1\varepsilon_{\mathrm{d1}}(\lambda) + K_2\varepsilon_{\mathrm{d2}}(\lambda)}{K_1 + K_2} \tag{26}$$

The minimization of σ_K by varying K was done in Microsoft Excel program using the Solver function, which allows one to minimize the content of one worksheet cell (σ_K) by varying values in other cells (K).

Acknowledgements

Z. P. was supported by Bader Fellowship. We are grateful to EPSRC, Grant GR/M 51000 for equipment used in this study. The usefull comments of Richard Ostler and Klaus Suhling are also greatfully acknowledged.

References

1 D. Phillips, Chemical mechanisms in photodynamic therapy with phthalocyanines, *Progress in Reaction Kinetics*, 1997, **22**, 3–4, 175–300.

2 A. Beeby, S. M. Bishop, H. G. Meunier, M. S. C. Simpson, and D. Phillips, Complexing of fluoride ions to disulphonated aluminium phthalocyanine, in *Photodynamic therapy and biomedical lasers*, eds. P. Spinelli, M. Dal Fante and R. Marchesini, Elsevier, Amsterdam, 1992, 732–736.

3 M. S. C. Foley, A. Beeby, A. W. Parker, S. M. Bishop and D. Phillips, Excited triplet state photophysics of the sulphonated aluminum phthalocyanine bound to human serum albumin, *J. Photochem. Photobiol. B*, 1997, **38**, 10–17.

4 S. Dhami, A. J. De Mello, G. Rumbles, S. M. Bishop, D. Phillips and A. Beeby, Phthalocyanine fluorescence at high concentration: dimers or reabsorption effect?, *Photochem. Photobiol.*, 1995, **61**, 341–346.

5 M. S. C. Foley, A. Beeby, A. W. Parker, S. M. Bishop and D. Phillips, Photophysics of disulphonated aluminum phthalocyanine in reverse micelles of Aerosol OT, *J. Photochem. Photobiol. B*, 1997, **38**, 18–24.

6 S. Dhami, J. J. Cosa, S. M. Bishop and D. Phillips, Photophysical characterization of sulfonated aluminum phthalocyanines in a cationic reversed micellar system, *Langmuir*, 1996, **12**, 2, 293–300.
7 S. Dhami, G. Rumbles, A. J. MacRobert and D. Phillips, Comparative photophysical study of disulfonated aluminum phthalocyanine in unilamellar vesicles and leukemic K562 cells, *Photochem. Photobiol.*, 1997, **65**, 1, 85–90.
8 S. Dhami and D. Phillips, Comparison of the photophysics of an aggregating and non-aggregating aluminium phthalocyanine system incorporated into unilamellar vesicles, *J. Photochem. Photobiol. A*, 1996, **100**, 1–3, 77–84.
9 M. Ambroz, A. J. MacRobert, J. Morgan, G. Rumbles, M. S. C. Foley and D. Phillips, Time-resolved fluorescence spectroscopy and intracellular imaging of disulphonated aluminium phthalocyanine, *J. Photochem. Photobiol. B*, 1994, **22**, 105–117.
10 A. L. Plant, Mechanism of concentration quenching of a xanthene dye encapsulated in phospholipid liposomes, *Photochem. Photobiol.*, 1986, **44**, 4, 453–459.
11 R. F. Chen and J. R. Knutson, Mechanism of fluorescence concentration quenching of carboxyfluorescein in liposomes: energy transfer to nonfluorescent dimers, *Anal. Biochem.*, 1988, **172**, 61–67.
12 A. D. Scully, A. Matsumoto and S. Hirayama, A time-resolved fluorescence study of electronic excitation-energy transport in concentrated dye solutions, *Chem. Phys.*, 1991, **157**, 1–2, 253–269.
13 K. Nakamura, T. Kowaki, A. D. Scully and S. Hirayama, Quenching of chlorophyll *a* fluorescence by oxygen in highly concentrated solutions and microdroplets, *J. Photochem. Photobiol. A*, 1997, **104**, 1–3, 141–149.
14 M. Sikorski, E. Krystkowiak and R. P. Steer, The kinetics of fast fluorescence quenching processes, *J. Photochem. Photobiol. A*, 1998, **117**, 1–16.
15 C. S. Owen, Two dimensional diffusion theory: Cylindrical diffusion model applied to fluorescence quenching, *J. Chem. Phys.*, 1975, **62**, 8, 3204–3207.
16 D. D. Eads, B. G. Dismer and G. R. Fleming, A subpicosecond, subnanosecond and steady-state study of diffusion influenced fluorescence quenching, *J. Chem. Phys.*, 1990, **93**(2), 1136.
17 S. Jang, K. J. Shin and S. Lee, Effects of excitation migration and translational diffusion in the luminescence quenching dynamics, *J. Chem. Phys.*, 1995, **102**(2), 815–827.
18 H. C. Joshi, H. Mishra, H. B. Tripathi and T. C. Pant, Role of diffusion in excitation energy transfer: a time-resolved study, *J. Lumin.*, 2000, **90**, 17–25.
19 D. L. Andrews and G. Juzeliunas, The range dependence of fluorescence anisotropy in molecular energy transfer, *J. Chem. Phys.*, 1991, **95**(8), 5513–5518.
20 M. Ambroz, A. Beeby, A. J. MacRobert, M. S. C. Simpson, R. K. Svensen and D. Phillips, Preparative, analytical and fluorescence spectroscopic studies of sulphonated aluminium phthalocyanine photosensitisers, *J. Photochem. Photobiol., B*, 1991, **9**, 87–95.
21 D. V. O'Connor and D. Phillips, *Time-correlated single-photon counting*, Academic Press, London, 1984.
22 P. W. Atkins, *Physical Chemistry*, Oxford University Press, Oxford, 1990, p. 689.
23 R. B. Ostler, An investigation of intracellular PDT mechanisms, PhD thesis, University of London, 1997.
24 R. B. Ostler, A. D. Scully, A. G. Taylor, I. R. Gould, T. A. Smith, A. Waite and D. Phillips, The effect of pH on the photophysics and photochemistry of disulphonated aluminium phthalocyanine, *Photochem. Photobiol.*, 2000, **71**, 4, 397–404.
25 R. S. Knox, Spectral effects of exciton splitting in "statistical pairs", *J. Phys. Chem.*, 1994, **98**, 7270–7273.
26 *CRC Handbook of Chemistry and Physics*, ed. D. R. Lide, CRC Press Inc., 1995.
27 T. Tao, Time-dependent fluorescence depolarization and brownian rotational diffusion coefficients of macromolecules, *Biopolymers*, 1969, **8**, 609–632.
28 G. S. Beddard, S. E. Carlin and G. Porter, Concentration quenching of chlorophyll fluorescence in bilayer lipid vesicles and liposomes, *Chem. Phys. Lett.*, 1976, **43**(1), 27–32.
29 M. S. C. Simpson, A. Beeby, S. M. Bishop, A. J. MacRobert, A. W. Parker and D. Phillips, Time resolved spectroscopic studies of sulphonated aluminium phthalocyanine triplet states, *Proc. SPIE-Int. Soc. Opt. Eng.*, 1992, **1640**, 520–529.